

CIRCUMFERENTIAL SURFACE CRACKS IN PIPES

Andrea Carpinteri*, Roberto Brighenti* and Andrea Spagnoli*

A circumferential external surface flaw in a metallic round pipe under constant amplitude cyclic bending loading is analysed. The defect is assumed to present an elliptical-arc shape with aspect ratio $\alpha = a_{el}/b_{el}$, while the relative depth ξ of the deepest point on the crack front is equal to the ratio between the maximum crack depth a_{el} and the pipe wall thickness t . The parameter R/t , with R = internal radius of the pipe, is equal to 10. The stress-intensity factor variation along the crack front is determined through a finite element analysis. Finally the fatigue propagation patterns in the diagram of α against ξ are theoretically obtained.

INTRODUCTION

The behaviour of surface cracks in plates and round bars has been analysed by several authors (for example, Carpinteri (1-4)), but only few studies have been carried out on circumferential edge flaws in pipes (Delale and Erdogan (5), Forman and Shivakumar (6), Raju and Newman (7) and Bergman (8)).

A circumferential external surface flaw is assumed to exist in the centre-line cross section of a metallic round pipe subjected to a constant amplitude cyclic bending loading. The defect presents an elliptical-arc shape with aspect ratio $\alpha = a_{el}/b_{el}$ (Fig.1), whereas the relative depth ξ of the deepest point A on the crack front is equal to the ratio between the maximum crack depth a_{el} and the wall thickness t of the pipe. The ratio R/t between the internal radius of the pipe and the wall thickness is assumed to be equal to 10. The aspect ratio α is made to vary from 0.0 to 1.2, while the relative crack depth ξ ranges from 0.05 to 0.8.

* Department of Civil Engineering, University of Parma
Viale delle Scienze, 43100 Parma, Italy

A finite element analysis is carried out with 20-node brick elements to calculate the stress-intensity factor variation along the crack front. Then the fatigue crack growth is examined by means of a theoretical model. The problem is complex since the flaw is an elliptical arc during the whole propagation, but the aspect ratio changes.

FINITE ELEMENT ANALYSIS

The stress field for the part-through cracked pipe under bending loading is determined by means of a finite element analysis. Because of symmetry, only one-fourth of the flawed structural component is modelled by 20-node isoparametric solid elements. A total of 3731 nodes and 720 finite elements are employed (Fig.2). The pipe sizes are assumed to be equal to D = external diameter = 50 mm and l = half-length = 200 mm.

Since the stress square-root singularity near the flaw is obtained by using quarter-point finite elements, reliable results cannot be deduced in a boundary layer near the intersection point B between crack front and external surface (Fig.1), but this effect is confined in a small region near point B (1). Therefore, only the results for ζ/h from 0.10 (point C) to 1.00 (point A) are considered in the following.

The dimensionless stress-intensity factor $\tilde{K}_{I,M}$ along the elliptical-arc crack front is calculated as follows :

$$\tilde{K}_{I,M} = \frac{K_{I,M}}{\sigma_M (\pi a_{e1})^{1/2}} \quad (1)$$

where

$$\begin{aligned} K_{I,M} &= \text{stress-intensity factor for tension} = \sigma_{Z,M} (2\pi r)^{1/2}, \\ &\quad \text{with } r \rightarrow 0, \\ \sigma_{Z,M} &= \text{opening stress (perpendicular to the crack plane) at the} \\ &\quad \text{distance } r \text{ from the generic point } P \text{ on the crack front,} \\ &\quad \text{with } r \text{ evaluated perpendicular to the front (Fig.1),} \\ \sigma_M &= M / [\pi ((D/2)^4 - R^4) / D] = \text{maximum bending stress.} \end{aligned}$$

The stress-intensity factor $\tilde{K}_{I,M}$ along the crack front is plotted in Fig.3 for different values of ξ . For circular-arc front ($\alpha = 1.0$), the maximum stress-intensity factor is attained near the external surface. On the contrary, all the dashed curves, which are related to the case of straight-fronted crack ($\alpha = 0.0$), increase by increasing the parameter ζ/h and, therefore, present the maximum value at point A.

Figure 4 shows the transition from $\alpha = 0.0$ to $\alpha = 1.2$ for $\xi = 0.3$. The slope of the curve $\tilde{K}_{I,M}$ becomes negative for α greater than or equal to about 1.0, that is to say, the maximum stress-intensity factor is attained at point A for $\alpha \leq 1.0$ and near point B for $\alpha \geq 1.0$. This transition phenomenon can also be observed for other values of relative crack depth, but the change of slope sign occurs in correspondence to a value of aspect ratio which decreases by increasing ξ . The results discussed in the present Section are quite close to those of other Authors (7,8).

FATIGUE PROPAGATION MODEL

As is well-known, the part-through cracks in flat plates tend to follow preferred fatigue propagation paths, that is, the crack aspect ratio is a function of the relative depth (crack depth / plate thickness) for both axial and bending cyclic loading (Burch (9), Mahmoud (10) and Carpinteri (11,12)). An analogous conclusion has also been drawn for edge flaws in round bars (Carpinteri (13,14)).

A theoretical model to analyse the growth of circumferential external surface flaws in pipes under cyclic bending is proposed. Since the ellipse centre is assumed to lie on the external perimeter of the pipe cross-section during the whole propagation (Fig.5), the generic crack front after one cyclic loading step can be expressed by the following equation:

$$\frac{x^2}{(b_{el}^*)^2} + \frac{y^2}{(a_{el}^*)^2} = 1 \quad (2)$$

where the two unknowns a_{el}^* and b_{el}^* can be obtained from the condition that the coordinates of the points A* and C*, deduced from the Paris-Erdogan law, must satisfy eqn(2).

Figure 6 displays the propagation patterns for surface flaws under cyclic bending with stress range $\Delta\sigma_M = 100 \text{ Nmm}^{-2}$. The material constants in Paris-Erdogan equation are assumed to be $m = 2$ and $A = 1.64 \times 10^{-10}$, for da/dN in mm cycle^{-1} and $\Delta K_{I,M}$ in $\text{Nmm}^{-3/2}$. The initial flaws examined have relative depth ξ_0 equal to 0.05, 0.10 or 0.20 and crack aspect ratio α_0 equal to 0.001 (straight front), 0.3, 0.5 or 1.0 (circular front). It can be remarked that, for each initial crack configuration being considered (ξ_0, α_0), the propagation path in the diagram of α against ξ tends to converge to a horizontal asymptote, with α included in the range 0.9 ~ 1.0.

CONCLUSIONS

Circumferential external surface flaws in metallic round pipes under cyclic bending loading with constant amplitude have been examined. The following conclusions can be drawn in the case of thin-walled pipes ($R/t = 10$, where R and t are the internal radius and the wall thickness of the pipe, respectively) :

- (1) For a given value of the relative crack depth $\xi = a_{el}/t$, the stress-intensity factor variation along the crack front is remarkably dependent on the flaw aspect ratio $\alpha = a_{el}/b_{el}$.
- (2) A two-parameter theoretical model has been proposed to analyse the fatigue growth of the surface defects being considered. For each initial crack configuration, the propagation path converges to a horizontal asymptote in the diagram of α against ξ , with α included in the range $0.9 \sim 1.0$.

ACKNOWLEDGEMENTS

The authors gratefully acknowledge the research support for this work provided by the Italian Ministry for University and Technological and Scientific Research (MURST) and the Italian National Research Council (CNR).

REFERENCES

- (1) Carpinteri, A. (Editor), "Handbook of Fatigue Crack Propagation in Metallic Structures", Elsevier Science Publishers B.V., Amsterdam, The Netherlands, 1994.
- (2) Carpinteri, A., Engng Fracture Mech., Vol.38, 1991, pp. 327-334.
- (3) Carpinteri, A., Fatigue Fracture Engng Mater. Struct., Vol. 15, 1992, pp. 1141-1153.
- (4) Carpinteri, A., J. Strain Anal. for Engng Design, Vol. 28, 1993, pp. 117-123.
- (5) Delale, F. and Erdogan, F., J. Appl. Mech., Vol. 49, 1982, pp. 97-102.
- (6) Forman, R.G. and Shivakumar, V., "Growth behavior of surface cracks in the circumferential plane of solid and hollow cylinders", In "Fracture Mechanics : Seventeenth Volume", ASTM STP 905, pp. 59-74, 1986.
- (7) Raju, I.S. and Newman, J.C., "Stress intensity factors for circum-

ferential surface cracks in pipes and rods", In "Fracture Mechanics : Seventeenth Volume", ASTM STP 905, pp. 789-805, 1986.

- (8) Bergman, M., Fatigue Fracture Engng Mater. Struct., Vol. 18, 1995, pp. 1155-1172.
- (9) Burch, L.H., Engng Fracture Mech., Vol. 9, 1977, pp. 389-395.
- (10) Mahmoud, M.A., Engng Fracture Mech., Vol. 36, 1990, pp. 389-395.
- (11) Carpinteri, A., Fatigue Fracture Engng Mater. Struct., Vol. 15, 1992, pp. 365-376.
- (12) Carpinteri, A., Int. J. Computers & Struct., Vol. 44, 1992, pp. 1317-1338.
- (13) Carpinteri, A., Int. J. Fatigue, Vol. 15, 1993, pp. 21-26.
- (14) Carpinteri, A. and Brighenti, R., Int. J. Fatigue, Vol. 18, 1996, pp. 33-39.

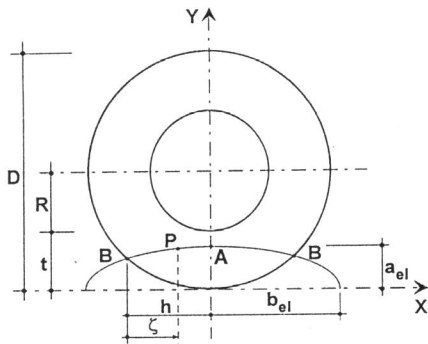


Fig. 1. Circumferential external surface flaw in a round pipe.

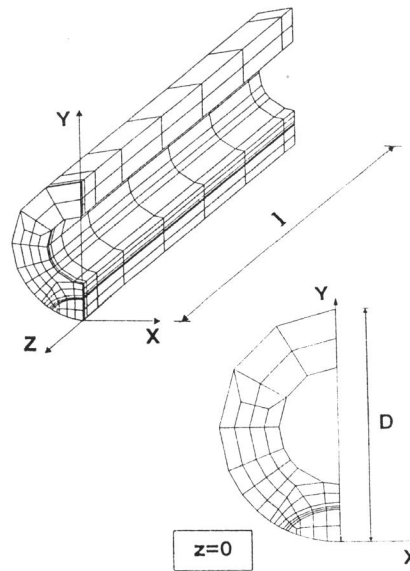


Fig. 2. Finite element mesh.

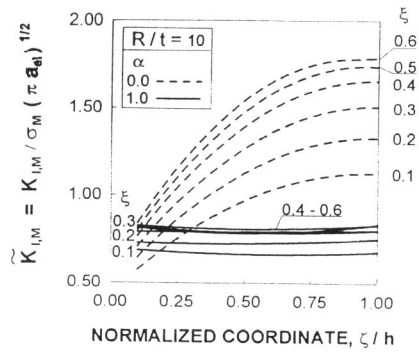


Fig. 3. Stress-intensity factor variation under bending, for $R/t = 10$.

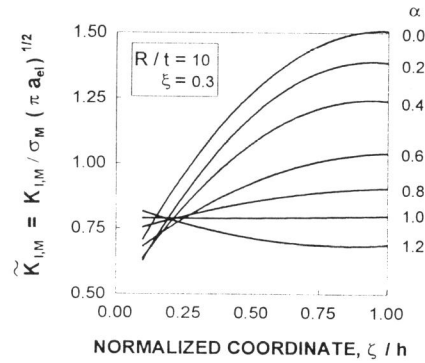


Fig.4. Influence of the crack aspect ratio α , for $R/t = 10$ and $\xi = 0.3$.

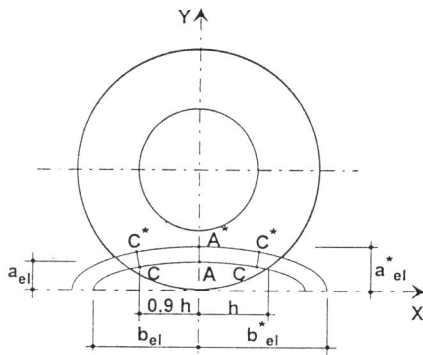


Fig. 5. Two-parameter model for fatigue crack propagation.

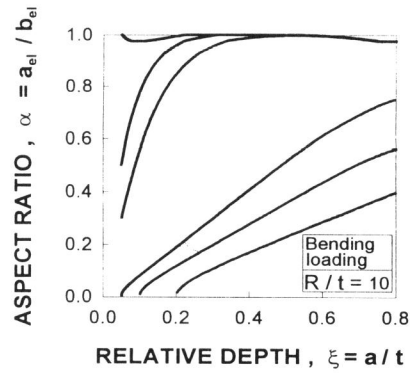


Fig. 6. Crack propagation paths under cyclic bending, for $R/t = 10$.